ELSEVIER

Cement & Concrete Composites 22 (2000) 353–360

Cement & Concrete Composites

www.elsevier.com/locate/cemconcomp

# Microcracking and chloride permeability of concrete under uniaxial compression

C.C. Lim [a], N. Gowripalan [a,*], V. Sirivivatnanon [b]

[a] School of Civil and Environmental Engineering, University of New South Wales, Sydney, NSW 2052, Australia
[b] CSIRO Building, Construction and Engineering, P.O. Box 310, North Ryde 1670, Australia

Received 28 February 2000; accepted 23 May 2000

**Abstract**

In the previous studies on microcracks and rapid chloride permeability tests, microcracks were quantified in terms of total crack length. This was carried out by examining concrete slices after compression tests. No attempts have been made to characterise the microcracks during the compression test prior to the chloride permeability test. In the present study, concrete cylinders were loaded under uniaxial compression between 30% and 95% of the ultimate strength. A non-destructive method of microcrack evaluation was used to study the progressive microcracking in concrete cylinders during compression tests. After the compression test, a rapid chloride permeability test (RCPT) (ASTM C1202) was carried out on a specimen cut from the same cylinder. The total crack length was also determined from the same specimen to compare with the observed microcracking behaviour, assessed by the non-destructive testing. The characteristics of the microcracks in terms of the specific crack area are different when a concrete is under a load and when it is completely unloaded. The chloride permeability of a concrete (after it was unloaded) appears to be influenced by the occurrence of a certain stress level known as the critical stress. When the critical stress is exceeded in a concrete specimen, a comparatively large chloride permeability was measured. Where the critical stress in a specimen is not exceeded, the increase in the permeability is marginal in spite of the large increase in microcracks. 

*Keywords:* Chloride permeability; Microcracking; Uniaxial compression; Rapid chloride permeability test; Specific crack area; Critical stress

## 1. Introduction

Microcracks are present in concrete due to several causes such as bleeding, shrinkage, thermal gradients, freeze-thaw and alkali-aggregate reaction [1]. Microcracks in concrete can also be induced by external loadings or as a result of the interaction of the concrete with the environment. Microcracks, which originally exist in the concrete, may propagate and become interconnected due to an applied stress [2]. These microcracks may form potential flow channels which provide easy access to aggressive salts and ions such as chloride ions. The importance of microcracks on the transport properties of concrete has been highlighted recently [3]. The effect of microcracking on permeability under uniaxial compression has been studied by several researchers [4–6]. However, there are some conflicting views pertaining to their findings.

Samaha and Hover [4] reported that microcracking in concrete at stress levels below 75% of the compressive strength did not affect the mass transport properties of concrete. The microcracks were quantified in terms of crack length by examining a concrete slice cut from a cylinder after the compression test. The observed crack length was then compared with the measured electrical charge passed using a rapid chloride permeability test (RCPT) carried out in accordance with ASTM C1202. On the other hand, Saito and Ishimori [5] found the chloride permeability of concrete that had been subjected to 90% of the compressive strength to be nearly equal to that of unloaded control specimens. However, he did not carry out microcrack evaluation on his specimens. He compared his permeability results with the microcracking behaviour of concrete reported by other researchers [8,16,17]. In this case, the interpretation of results may be dubious because of different microcracking conditions. Ludirdja et al. [6] reported that

* Corresponding author. Tel.: +61-2-9385-5146; fax: +61-2-9385-6139.
*E-mail address:* n.gowripalan@unsw.edu.au (N. Gowripalan).

0958-9465/00/$ - see front matter 
PII: S0958-9465(00)00029-9

Table 1
Concrete mix proportions

| Grade | Mix proportions (kg/m$^3$) | | | | w/c | $f'_c$ at 28 days (MPa) |
|---|---|---|---|---|---|---|
| | Cement | Water | Sand | c/agg | | |
| 40 | 390 | 180 | 810 | 988 | 0.46 | 47.5 |

compressive loads had little effect on the water permeability of concrete even though there were some indications of significant microcracking in the concrete. He did not carry out crack measurements but used an ultrasonic pulse velocity method to detect microcracking in concrete.

In the previous studies [4–6], no attempts had been made to characterise the microcracks during the compression test. It is evident that the characteristics of microcracks after a concrete has been unloaded are different from those while under load. Wang et al. [10], for example, introduced a feedback controlled splitting test to generate and characterise tensile cracks in a concrete specimen. He found that the crack opening displacement reduced after the load had been completely removed from the specimen. Loo [12] reported similar observations for concrete cylinders subjected to uniaxial compression tests. Microcracks in concrete begin to propagate under uniaxial compression between 15% and 45% of the compressive strength [7]. The microcracks become unstable at stresses between 70% and 90% of the compressive strength when they begin to propagate rapidly under a load [8,9]. In view of the wide range of stresses at which microcracks begin to propagate and at which microcracks become unstable, microcrack evaluation and RCPT shall ideally be carried out on the same concrete specimen. Therefore, it would be more appropriate to characterise the microcracks during the compression test so that a more realistic account of the influence of microcracks on the permeability of the concrete can be made.

In the present study, a non-destructive method of microcrack evaluation [7] is used to evaluate the progressive microcracking behaviour in the concrete cylinder under uniaxial compression test. The microcracks are characterised in terms of specific crack area which is defined as the increase in the crack area per unit cross-sectional area of the specimen [7]. This is described further in Section 2.2. After the compression test, an RCPT (ASTM C1202) was carried out on a specimen cut from the same cylinder. An estimate of the total crack length from the same specimen was also carried out to supplement the observed microcracking behaviour. Comparisons between the specific crack area, total crack length and the electrical charge passed through the specimen were made and discussed.

## 2. Experimental program

### 2.1. Preparation of specimens

Grade 40 concrete mix was designed using locally available Nepean crushed gravel and Nepean sand as coarse and fine aggregates, respectively. The concrete mix was prepared in accordance with the Australian Standard, AS1012. Both aggregates were pre-soaked in water before batching so that the moisture content was above the saturated-surface dry (SSD) condition. General Purpose cement (similar to ASTM Type I) complying with AS3972 was used. A water reducing admixture was added to achieve a slump of $100 \pm 20$ mm. The quantities of the mix proportions per cubic metre of concrete are shown in Table 1.

Concrete cylinders, $\varnothing 100\text{ mm} \times 200\text{ mm}$, were cast in two layers. Each layer was compacted using a vibrating table. After casting, the specimens were covered with plastic sheets. All mixing and casting were carried out in a standard laboratory condition at $23 \pm 2$°C and $50 \pm 5$% RH. The cylinders were demoulded on the following day and moist-cured in lime saturated water up to the age of 28 days.

### 2.2. Non-destructive method of microcrack evaluation

The non-destructive method of evaluation developed recently by Loo [7] was used to characterise the microcracks during the uniaxial compression test. The method provides a quantitative indication of the extent of microcracking in a concrete specimen during the test. The formula was derived on the assumption that the change in cross-sectional area of a prismatic concrete specimen under uniaxial compression is equal to the sum of the elastic change in cross-sectional area due to Poisson's ratio effects and the dilation due to microcracking, hence,

$$\Delta A_T = \Delta A_C + \Delta A_{PR}, \quad \text{(i)}$$

where $\Delta A_T$ is the total change in cross-sectional area of concrete, $\Delta A_C$ the change in cross-sectional area due to microcracking and $\Delta A_{PR}$ is the change in cross-sectional area due to Poisson's ratio effects. Based on this assumption, Loo [7] has shown that the specific crack area ($\varepsilon_{cr}$) can be estimated from

$$\varepsilon_{cr} = 2(\varepsilon_x - \mu_e \varepsilon_y), \quad \text{(ii)}$$

where $\varepsilon_x$ and $\varepsilon_y$ are the transverse and axial strains, respectively, and $\mu_e$ is the elastic Poisson's ratio. The specific crack area has the same unit as the $\varepsilon_x$ and $\varepsilon_y$, and is expressed in microstrain. For a circular specimen, the specific crack area is equal to $\Delta A_C/\pi r^2$. Four electrical strain gauges are required per specimen, two in each axial and transverse directions. The two strain gauges in the transverse direction are positioned at the mid-height of the specimen. Strain gauges with a gauge length of 30 mm and a gauge factor of $2.13 \pm 1\%$ were used.

After 28 days of casting, concrete cylinders were tested under uniaxial compression between $0.3f'_c$ and $0.95f'_c$. Upon reaching the predetermined stress level, unloading commenced immediately until the cylinder was completely unloaded. Recording of the strain data was continued until the recovery was negligible. A 2000 kN capacity Baldwin closed-loop servo controlled hydraulic compression machine was used for this test. A ram displacement rate of 0.09 mm/min for loading and 2.0 mm/min for unloading was adopted. All strain data from the electrical strain gauges were logged. For each stress level, microcrack evaluation was carried out on two concrete cylinders.

### 2.3. Rapid Chloride Permeability Test (RCPT)

At the end of the compression test, the strain gauges were removed from the concrete cylinder. A 50 mm-thick specimen was cut from the mid-height of the cylinder. This is shown schematically in Fig. 1. The specimen was air-dried before coating with epoxy on the circumferential surface. It was then vacuum-saturated in a vacuum desiccator. RCPT was carried out in accordance with ASTM C1202 [11]. The current was recorded every 15 min using a data logger. The chloride permeability of the concrete was evaluated by the amount of charge passing through the specimen.

### 2.4. Microscopy observation of microcracks

The 10 mm slice, cut just above the 50 mm thick specimen shown in Fig. 1, was used for microcrack examination under a microscope. It was stained with a red dye on the cut surface adjacent to the 50 mm thick specimen for RCPT. The specimen was subsequently polished with silicon carbide paper and water, on a glass plate, until the surface became pinkish in colour. At this stage, some larger bond cracks at the aggregate-paste interface were stained in deep red and could often be seen by the naked eye.

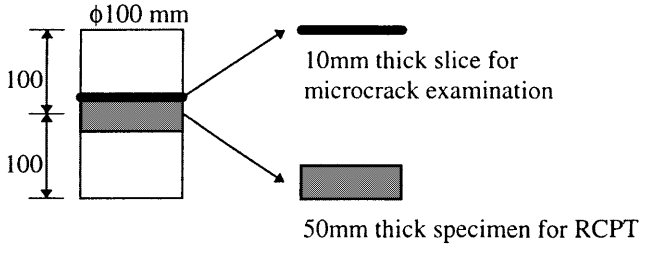


Fig. 1. Schematic diagram showing the specimens taken from a concrete cylinder for microcrack examination and rapid chloride permeability test.

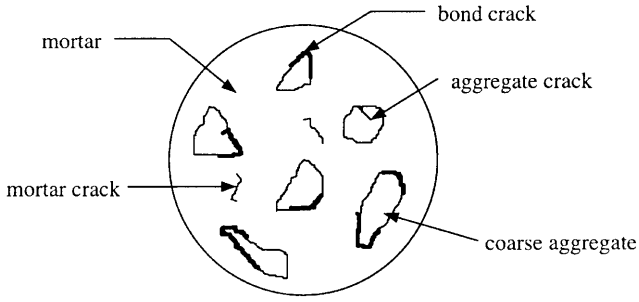


Fig. 2. A sketch showing the types of microcracks in concrete.

Enlarged photographs of polished specimens were taken. The specimen was then examined under an optical microscope using a magnification of between 20 and 40 times to observe for microcracks. The search for bond cracks was made using the microscope and the observed bond cracks were mapped on the enlarged photograph. After this, the same procedure was followed to detect the mortar and aggregate cracks. The crack length was estimated from the enlarged photograph by dividing the crack length into several straight segments. A sketch showing the types of microcracks in a concrete is shown in Fig. 2.

## 3. Results and discussion

### 3.1. Evaluation of specific crack area

Some results from the non-destructive tests are shown in Fig. 3. The initiation stress is the stress at which microcracks begin to propagate in concrete. This can be determined from the graphs in Fig. 3 as the point when the curve begins to deviate from the initial vertical line. In the present study, the initiation stress is found to be between $0.2f'_c$ and $0.4f'_c$. Fig. 3(b) and (c) show the characteristics of microcracks at $0.85f'_c$ in concrete where the critical stress is not exceeded in one instance and exceeded in the other, respectively.

In this series of tests, upon reaching the predetermined stress level, the specimen was unloaded immediately. Up to $0.5f'_c$ stress level, the specific crack area recovery is almost 100% as shown in Fig. 3(a). It implies that the microcracks close back almost completely upon complete unloading. However, at $0.7f'_c$ and above, some

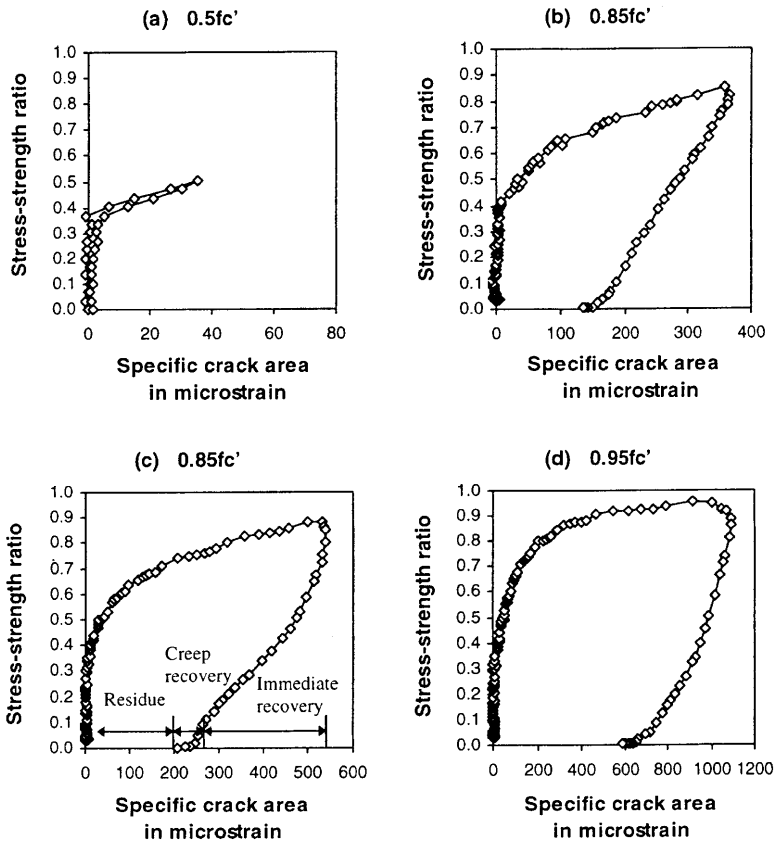


Fig. 3. Typical characteristics of microcracks in concrete at different compressive stress levels.

residue specific crack areas are observed after the concrete has been unloaded completely. This implies only a partial closure of the microcracks in the concrete. The residue specific crack area was determined after three days of the creep recovery.

The relationship between the specific crack area at predetermined stresses and their recovery immediately after complete unloading is shown in Fig. 4. The difference in the specific crack area between the two curves is the immediate recovery. It indicates the reduction in the area of microcracks per unit cross-sectional area of the concrete when the concrete is unloaded immediately from its predetermined stress level. This observation shows that the characteristic of microcracks, in terms of specific crack area, is indeed different from each other, when a concrete is loaded and when it is completely unloaded.

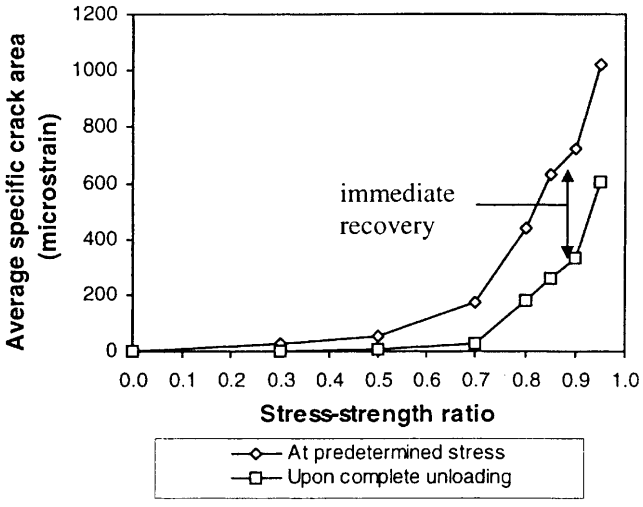


Fig. 4. Average specific crack area in concrete during loading and unloading in compression.

### 3.2. Critical stress

The critical stress, $\sigma_c$, represents the onset of unstable microcrack propagation [7]. It corresponds to the maximum value of volumetric strain ($\varepsilon_v = \varepsilon_1 + \varepsilon_2 + \varepsilon_3$), beyond which the specimen undergoes a volumetric expansion. Fig. 5 shows some typical curves of the axial, lateral and volumetric strains for specimens which have been loaded up to $0.95f'_c$ in the compression tests. In the present study, the critical stress is found to be exceeded in specimens that have been loaded between $0.8f'_c$ and $0.95f'_c$. However, there are some concrete cylinders

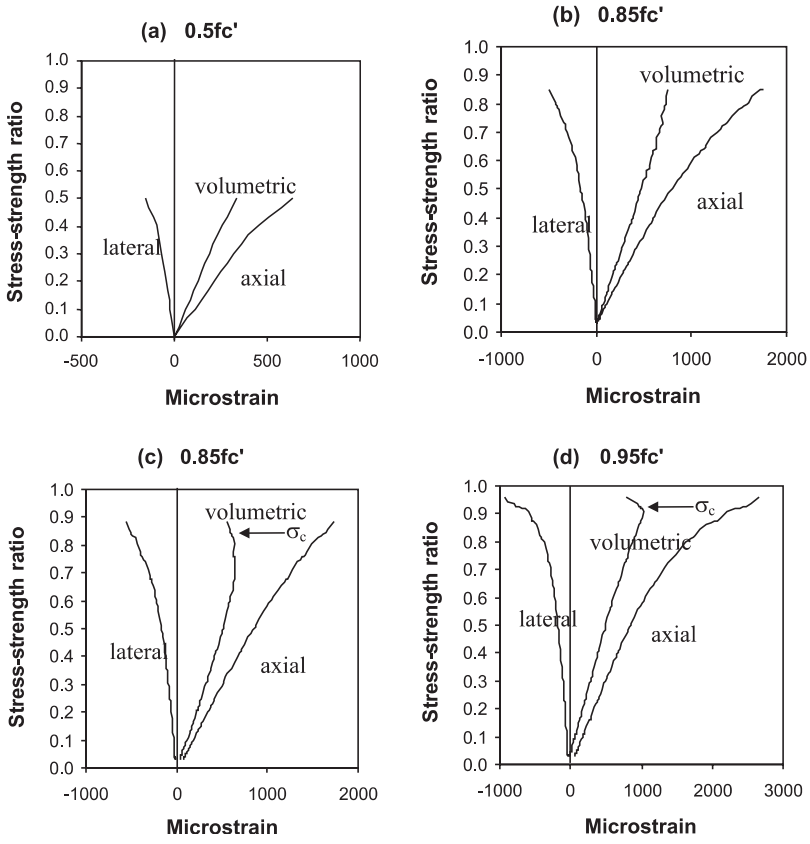


Fig. 5. Typical curves of axial, lateral and volumetric strains.

where the critical stress was not exceeded at $0.80f_c'$ and $0.85f_c'$. The critical stress is indicated by a horizontal arrow on the volumetric strain curve. Fig. 5(b) and (c) show the typical strain curves of concrete loaded up to $0.85f_c'$ where the $\sigma_c$ is not exceeded in one instance but is exceeded in the other.

### 3.3. Total crack length

Fig. 6 shows the relationship between the total crack length and the stress level. Each result is an average of observation made on two specimens. It is observed that there is virtually no increase in the total crack length below $0.3f_c'$. A marginal increase in the crack length is observed between $0.3f_c'$ and $0.5f_c'$. These are essentially bond cracks as they occur at the aggregate–mortar interface. Beyond $0.5f_c'$, the total crack length increases significantly. On the other hand, mortar cracks become noticeable above $0.7f_c'$. They were found as isolated cracks in the mortar at $0.7f_c'$ but become connected with some bond cracks in the specimen loaded to $0.9f_c'$ where the critical stress was found to be exceeded. Bond cracks were found to propagate into the mortar at $0.8f_c'$. At any stress level, the bond cracks are considerably more than

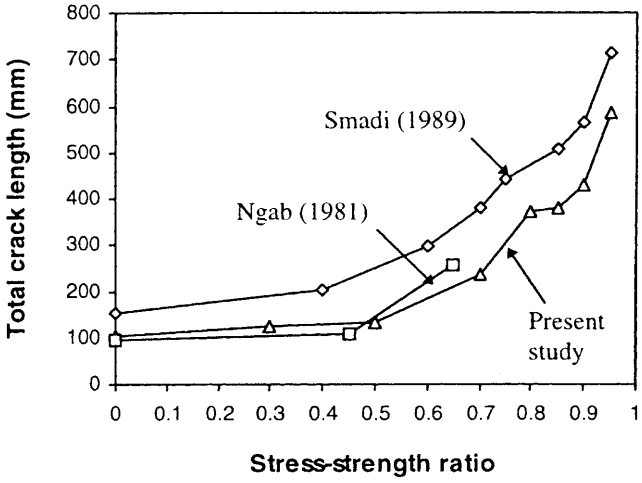


Fig. 6. Relationship between total crack length and stress-strength ratio.

the mortar cracks. Cracks through the aggregate were found to be insignificant at all stages of loading. Although some aggregate cracks were also observed, it was not certain if they were true cracks developed during loading or simply fissures. However, the quantity was very small and was ignored.

Some results of microcrack observations from the previous studies [14,15] are replotted in Fig. 6 for comparison. They are obtained from microcrack examination on normal strength concretes (33–41 MPa). Ngab et al. [14] reported a significant increase in cracking only at stress levels above $0.45f_c'$. Smadi and Slate [15] reported negligible increase in microcracking below $0.40f_c'$ but became significantly large at stresses above $0.70f_c'$. The total crack lengths are different among the various studies due to the different strength of concrete, mix proportions and the size of specimens used for crack count. The size of specimens used by Ngab et al. [14] and Smadi and Slate [15] was $89\times89$ mm$^2$ $\varnothing$102 mm, respectively. However, the microcrack observation in the present study shows a similar trend and is consistent with the previous works [13–15]. Typical cracking maps are shown in Fig. 7.

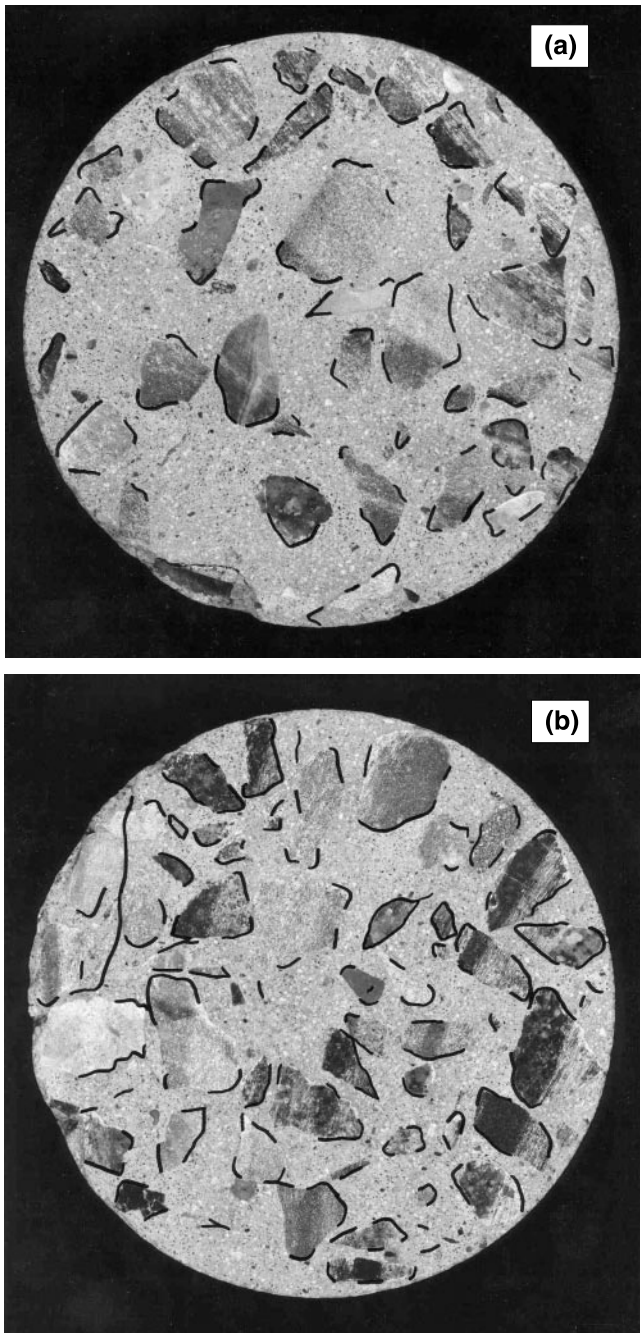


Fig. 7. Typical cracking maps: (a) $0.7f_c'$; (b) $0.95f_c'$.

### 3.4. RCPT

The results of RCPTs at different stress-strength ratio are shown in Fig. 8. The measured charge passed on all the test specimens is normalised against the charge passed through unloaded control specimens. Each result being an average of two specimens.

At stress levels below $0.5f_c'$, there is no apparent increase in the charge passed when compared with the unloaded control. This can be attributed partly to the closure of the microcracks when the specimen was unloaded completely, as depicted in Fig. 3(a). The immediate recovery from $0.3f_c'$, for example, was found to be about 25 microstrain with zero residue specific crack area (Fig. 4). This shows that the microcracks closed back completely when the specimen was unloaded from $0.3f_c'$. It is believed that there might not be any difference in the crack length at $0.3f_c'$ and when unloaded completely. However, the specific crack area does in fact vary. It appears that the influence of microcracks on mass transport in concrete cannot be depicted by its crack length only. Depending on the stress level at which the concrete is subjected, microcracks can close back partially or completely upon unloading. This is evident from the immediate recovery in Fig. 4. The ability of the microcracks to 'open' and 'close' may suggest that the

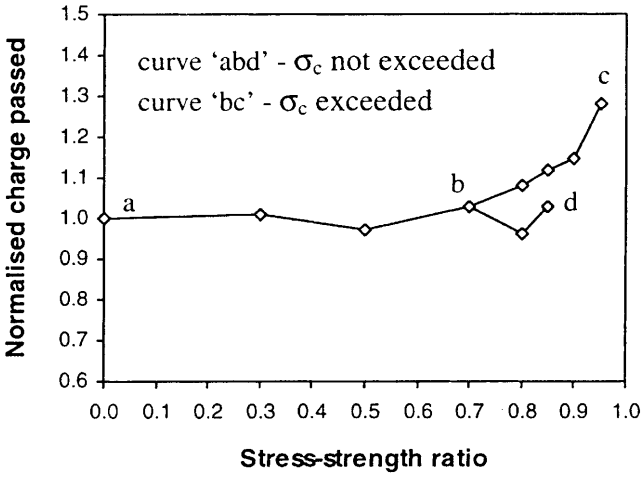


Fig. 8. Rapid chloride permeability results at different stress-strength ratio.

specific crack area is a more sensitive parameter to consider than the crack length, when relating permeability to stresses in concrete. The permeability of concrete can, thus, be influenced by the test condition i.e., whether the test was carried out under loading condition or after removal of load. Further work is needed to confirm this.

At $0.7f_c'$, the increase in crack length is substantial at 125% when compared with that of the unloaded control. However, the normalised charge passed (Fig. 8) appears marginal. A possible reason for this would be that the critical stress is not exceeded at $0.7f_c'$. The inter-connectivity of the microcracks in the concrete matrix appears to be another factor influencing the charge passed in a RCPT. In the present study, when the critical stress is exceeded, a comparatively large charge passed was measured. There are two stress levels, beyond $0.7f_c'$, where the critical stress was exceeded in some specimens and not exceeded in other specimens. As shown in Fig. 8, a comparison between the charges passed at $0.80f_c'$ and $0.85f_c'$ clearly shows the influence of the occurrence of critical stress on the permeability of the concrete.

From the literature, there is conflicting evidence as to how stress level affects chloride permeability of concrete. Samaha and Hover [4], for example, reported a low average charge passed for stress levels below $0.75f_c'$ despite a considerable increase in the crack length at $0.75f_c'$ when compared with the unloaded control. He found the charge passed to be more pronounced when the concrete was loaded to its full compressive strength. In contrast, Saito and Ishimori [5] reported negligible increase in the chloride permeability at $0.9f_c'$ when compared with his unloaded control. In both studies, no attempt was made to determine the critical stress occurrence in their test specimens.

Based on the observation made in the present study, the conflicting views can be explained in terms of the occurrence of the critical stress in the specimen. The increment of stress level considered beyond $0.7f_c'$ is small to ensure that useful observations are not eluded. In the present study, the increase in the total crack length is notably high at $0.80f_c'$ and $0.85f_c'$ although the critical stress is not exceeded. However, a comparatively higher charge passed is observed only when the critical stress is exceeded at these stress levels. Therefore, the low charges passed at $0.75f_c'$ [4] and at $0.9f_c'$ [5] can be attributed to the critical stress not being exceeded in the specimens. The wide range of critical stress in concrete should be considered in addition to the strength variability.

The results of chloride permeability observed in the present study are based on tests conducted on specimens after it has been completely unloaded. Further research is needed to study the chloride permeability through concrete specimens under load.

## 4. Conclusions

1. In a uniaxial compression test, when a concrete specimen is unloaded completely from $0.5f_c'$ stress level, the specific crack area recovery is 100% implying that microcracks close back completely. However, when unloaded between $0.7f_c'$ and $0.95f_c'$ stress level, some residue specific crack areas are observed immediately after complete unloading. This implies only a partial closure of the microcracks.
2. It appears that the influence of microcracks on mass transport in concrete cannot be depicted by its crack length only. Depending on the stress level at which the concrete was subjected, microcracks can close back partially or completely upon unloading. The ability of the microcracks to 'open' and 'close' may suggest that the specific crack area is a more sensitive parameter to consider than its crack length, when relating permeability to stresses in concrete.
3. In the present study, the critical stress is found to be exceeded when the concrete cylinders are loaded to a stress level between $0.80f_c'$ and $0.95f_c'$. However, there are some specimens where the critical stress is not exceeded when tested at $0.80f_c'$ and $0.85f_c'$.
4. The chloride permeability of a concrete (after it is unloaded) appears to be influenced by the occurrence of the critical stress. When the critical stress is exceeded in a concrete specimen, a comparatively large electrical charge passed was measured. Where the critical stress in a specimen is not exceeded, the increase in the charge passed is marginal in spite of the large increase in microcracks.
5. The chloride permeability of a concrete may be influenced by the test condition, i.e., whether the test was carried out under loading condition or after removal of load. Further work is needed to confirm this.

## Acknowledgements

The authors gratefully acknowledge the facilities and partial financial support from CSIRO Building, Construction and Engineering, Sydney, Australia for this research project.

## References

[1] Mehta PK. Concrete Technology at the Crossroads – Problems and Opportunities. Concrete Technology: Past, Present and Future. Proceedings of VM Malhotra Symposium, ACI SP144. MI: Detroit, 1994. p. 1–30.
[2] Mehta PK. Durability – critical issues for the future. Concrete Int 1997:27–33.
[3] Rostam S. High performance concrete cover – why it is needed and how to achieve it in practice. Construction Building Mater 1996;10(5):407–21.

[4] Samaha HR, Hover KC. Influence of microcracking on the mass transport properties of concrete. ACI Mater J 1992;89(4): 416–24.
[5] Saito M, Ishimori H. Chloride permeability of concrete under static and repeated compressive loadings. Cement Concrete Res 1995;25(4):803–8.
[6] Ludirdja D, Berger RL, Young JF. Simple method for measuring water permeability of concrete. ACI Mater J 1989;86(5):433–9.
[7] Loo YH. A new method for microcrack evaluation in concrete under compression. Mater Struct 1992;25:573–8.
[8] Hsu TTC, Slate FO, Sturman GM, Winter G. Microcracking of plain concrete and the shape of the stress–strain curve. ACI J 1963;60(2):209–24.
[9] Mehta PK, Monteiro PJM. Concrete: structures, properties and materials. Englewood Cliffs, NJ: Prentice Hall, 1993. p. 548.
[10] Wang K, Jansen DC, Shah SP. Permeability study of cracked concrete. Cement Concrete Res 1997;27(3):381–93.
[11] ASTM C 1202-97. Standard test method for electrical indication of concrete's ability to resist chloride ion penetration. Philadelphia: American Society for Testing and Materials, 1997.
[12] Loo YH. Propagation of microcracks in concrete under uniaxial compression. Magazine Concrete Res 1995;47(170):83–91.
[13] Najjar WS, Hover KC. Neutron radiography for microcrack studies of concrete cylinders subjected to concentric and eccentric compressive loads. ACI Mater J 1989;86(4):354–9.
[14] Ngab AS, Slate FO, Nilson AH. Microcracking and time-dependent strains in high-strength concrete. ACI J 1981:262–68.
[15] Smadi MM, Slate FO. Microcracking of high and normal strength concretes under short and long term loadings. ACI Mater J 1989;86(2):117–26.
[16] Krishnaswamy KT. Strength and microcracking of plain concrete under triaxial compression. ACI J 1968;65(10):856–62.
[17] Shah SP, Chandra S. Critical stress, volume change and microcracking of concrete. ACI J 1968:770–80.